



ELSEVIER

Available online at www.sciencedirect.com

SCIENCE @ DIRECT®

Earth and Planetary Science Letters 232 (2005) 315–332

EPSL

www.elsevier.com/locate/epsl

A negative fold test on the Lorrain Formation of the Huronian Supergroup: Uncertainty on the paleolatitude of the Paleoproterozoic Gowganda glaciation and implications for the great oxygenation event

Isaac A. Hilburn^a, Joseph L. Kirschvink^{a,*}, Eiichi Tajika^b, Ryuji Tada^b,
Yozo Hamano^b, Shinji Yamamoto^b

^a*Division of Geological and Planetary Sciences, California Institute of Technology, Pasadena, California 91125, USA*

^b*Department of Earth and Planetary Science, University of Tokyo, 7-3-1 Hongo, Tokyo 113-0033, Japan*

Received 18 December 2003; received in revised form 4 September 2004; accepted 27 November 2004

Available online 13 March 2005

Editor: V. Courtillot

Abstract

Previous paleomagnetic studies of the glaciogenic Gowganda and Lorrain formations have identified several low-inclination magnetic components of high thermal stability, which suggest low-latitude glaciation during deposition of the Huronian Supergroup, Canada. While extraordinary claims demand extraordinary proof, prior authors have been unable to support their interpretations of these components conclusively with any of the classic field stability tests (e.g., conglomerate, fold, and baked contact) capable of demonstrating that the magnetization was acquired at or soon enough after the time of deposition to be used to constrain the paleolatitude of the Gowganda or Lorrain formations. We report here the results of a fold test from the “purple siltstone” member of the Lorrain Formation near the town of Desbarats, Ontario, which indicate that none of the reported components dates to the time of deposition. Hence, the paleolatitude of the Gowganda glaciation is uncertain.

Comparison of the lithostratigraphic, paleomagnetic, and radiometric constraints on the Huronian sequence and the Transvaal Supergroup of Southern Africa implies that the one verified low-latitude Paleoproterozoic glacial event (the Makganyene glaciation, Transvaal Supergroup, South Africa) is younger than the three glacial units of Canada. With this correlation, the physical rock record indicates that the ‘great oxygenation event’ began in the time interval between the Gowganda and Makganyene glaciations. These data are consistent with the sudden evolution of oxygenic photosynthesis destroying a methane greenhouse and thereby triggering the first Snowball Earth event in Earth history.

© 2005 Elsevier B.V. All rights reserved.

Keywords: Huronian Supergroup; paleomagnetism; Snowball Earth; Paleoproterozoic glaciations; The great oxygenation event; Superior Province; apparent polar wander; Paleoproterozoic climate

* Corresponding author.

E-mail address: kirschvink@caltech.edu (J.L. Kirschvink).

1. Introduction

One of the major contributions of paleomagnetic studies to the field of paleoclimatology has been to provide constraints on the latitude of Proterozoic glacial intervals. As reviewed recently by Evans [1], several tightly constrained results for the Neoproterozoic that indicate the presence of tropical glaciers near the equator have lent support to the much-debated ‘Snowball Earth’ hypothesis [2–5]. In contrast, of the several studied Paleoproterozoic glaciogenic units, only the Makganyene and Ongeluk formations [6] from the Transvaal Supergroup of South Africa are constrained directly by a paleomagnetic field test of stability. Although two recent studies of the youngest glacial interval in the Huronian Supergroup of Canada [7,8] isolated high-temperature, low-inclination magnetic components, the authors were unable to conduct conclusive field stability tests to constrain more precisely the time at which the magnetizations were acquired.

In these papers, Williams and Schmidt [7] and Schmidt and Williams [8] isolated high-temperature, low-inclination components from the Gowganda Formation, which is glacial marine to post-glacial, and the Lorrain Formation, which is deltaic and fluvial, in the Upper Huronian Supergroup of Canada. In particular, a purple siltstone member from the Lorrain near the town of Desbarats yielded a high-temperature, low-inclination component, termed “Lorrain-A.” Although the single fold test conducted on this component proved inconclusive, based upon the facies and mineralogy of the Lorrain “purple siltstone” red beds and the tentative presence of normal and reversed “Lorrain-A” components the authors interpreted the component as a chemical remanent magnetization (CRM) acquired soon after deposition. Upon examination of one of their sampling localities, we located a small-scale chevron fold with an ideal orientation for performing a fold test on this component. Our results support the interpretation of the Lorrain-A as a CRM, but they also indicate that the component does not provide sufficient constraints on the Upper Huronian paleolatitude to justify a claim of low-latitude glaciation for the Gowganda.

Unlike the Paleoproterozoic Makganyene event of Southern Africa [9], the three Huronian glacial intervals do not have associated geological features

that make sense in the context of ‘hard’ Snowball Earth events [10,11], so they may be more akin to Phanerozoic glaciations.

2. Study site and geology

The Huronian Supergroup is subdivided into four groups: Elliot Lake, Hough Lake, Quirke Lake, and Cobalt, the interior makeup and genesis of which are related to a possible Wilson cycle [12]. The stratigraphy of the Huronian is bounded above and below by dated intrusives and volcanics. The Matachewan dyke swarm is contained in the Thessalon Fm, a volcanic unit of the Elliot Lake group, and provides a range of U–Pb ages between 2473 and 2446 Ma for the basal Huronian [13–16]. The Nipissing Diabases, a series of mafic sills and dykes, intrude up through the entire Huronian Supergroup and provide an upper age constraint of 2219 ± 4 Ma [17]. For comparison, the Ongeluk flood basalts in South Africa, which conformably overlie and interfinger with the Makganyene diamictites, have yielded a Pb–Pb age of 2222 ± 13 Ma [18]. They also contain detrital zircons as young as 2225 ± 3 Ma [19].

The three upper units in the Huronian comprise a repeated cycle. Each unit begins with glaciogenic diamictites—the Ramsay Lake, Bruce, and Gowganda formations—succeeded by mudstones and/or carbonates, siltstones, and cross-bedded sandstones [12]. Young and Nesbitt [20] proposed that the rocks of the first two cycles were deposited in a restricted basin and that subsequent rifting allowed for a widespread deposition of the upper Cobalt Group on a passive continental margin. Stratigraphically, the lowermost unit in the Cobalt Group, the Gowganda Formation, unconformably overlies the Serpent Formation of the Quirke Lake Group. The basal Coleman member of the Gowganda Formation contains a glacial diamictite with pebble to boulder-sized Archean granitic and meta-volcanic clasts and a dark silty to sandy matrix [20–23]. Feng et al. [24] noted a lack of Fe and Mg in alteration rinds on many of the granitic clasts in the Coleman member, which they interpreted as evidence for the absence of oxygen in soil waters, and therefore in the atmosphere, at the time of deposition (~2.3 Ga). The Firstbrook member of the Gowganda Fm overlies the Coleman and consists primarily of pink and red

hued siltstone and argillite that have been noted as possible evidence for the presence of atmospheric oxygen [22]. The Lorrain Formation conformably overlies the Gowganda Formation and consists primarily of arkosic sandstones and coarse, granule-pebble conglomerates, with several minor siltstone members [12,22]. Regionally, the Lorrain also overlies a ca. 2.45–2.2 Ga paleosol developed on Archean granites and meta-volcanics. Enrichment of ferric iron in these paleosols has been interpreted by Prasad and Roscoe [25] as evidence for atmospheric oxygen at or just prior to the deposition of the Lorrain and Cobalt groups. Several of the Lorrain units are red to purple in color and contain hematite and magnetite [7]. Other studies have flagged the Lorrain Fm as containing some of the oldest fluvial red beds and are supposedly an early indicator of atmospheric oxygen [10,22,26]. The “purple siltstone” member from which we sampled is a grayish red purple (~5RP 4/2) fine- to medium-grained silty sandstone located in the Lorrain Formation. (All color designations are from the Geological Society of American Rock Color Chart, 1963.)

3. Previous paleomagnetic studies on Huronian rocks

Over the past 30 yrs, a substantial number of studies have been conducted on the magnetic properties and remanent magnetization of various units—the Matachewan dyke swarm [13], the Nipissing sills [27], and the Lorrain and Gowganda formations [7,8]—within the Huronian Supergroup, and the Southern and Superior Provinces.

Buchan reported a low-latitude, southwesterly, primary remanent magnetization, M (Table 1a), for the Matachewan dyke swarms in samples from 17 different sites near Kirkland lakes on the boundary between the Superior and Southern Provinces [27]. A baked-contact test of the Matachewan cross-cutting into the older Otto stock dyke swarms (U–Pb age of 2680 ± 1 Ma) confirms the primary nature of this magnetization [13].

Buchan [27] also conducted a baked-contact test on the “N1” component of the Nipissing diabases from sites near Everett Lake, 4 km northeast of the town of Gowganda on the Cobalt plate. He sampled from six

sites, two located within the Nipissing sills and four located in the crosscutting Matachewan dykes at increasing distance from the sills. The two sill sites and the nearest dyke site yielded the “N1” direction (Table 1a), whereas the three farther sites yielded directions compatible with the Matachewan direction reported in Buchan [27], which confirms the primacy of the “N1” component in the Southern Province.

Buchan et al. [28] also conducted a baked-contact test on the “N3” component (Table 1a) of the Nipissing diabases from sites near Wendigo Lake, Englehart, Ontario. They sampled from multiple sites in the Nipissing diabases and neighboring sediments of the Coleman member, basal Gowganda Formation. The results of the baked-contact test were inconclusive, as the authors were unable to isolate any reliable and stable pre-Nipissing component from the Coleman sediments. The results, however, do suggest that the “N3” component was acquired before the intrusion of a local Biscotasing dyke (inferred from Buchan et al. [29,30]).

At one locality (Site 8310) in the Coleman red beds located ~1 km southwest of an intruding Nipissing dyke, the authors isolated a high-temperature (>600 °C), low-inclination component (Coleman-C) unlike any of the Nipissing directions [28]. At two separate sites located >1 km away and north of the Nipissing dyke (on the opposite side from Site 8310), they sampled 14 Archean mafic and granitic cobbles from the basement rock underlying the Coleman red beds to perform a conglomerate test on the Coleman-C direction. Based upon the random scatter in directions obtained, the authors concluded that Coleman site 8310 had not been thermally overprinted. However, as their clasts were not of the same or similar lithologies as the Coleman red beds and were located geographically quite distant from Site 8310, the test places no useful constraint on the Coleman-C remanence.

Williams and Schmidt [7] sampled the Coleman diamictite, sandstone, and argillite near Cobalt, Latchford, Temagami, Elliot Lake, Cumming Lake, and Gowganda, the Firstbrook siltstone member near Cobalt and Latchford, and the Lorrain “purple siltstone” member from multiple sites near Desbarats. Four components, Coleman-sandstone-A, Coleman-sandstone-B, Coleman-diamictite-A, and Coleman-diamictite-B were isolated from seven sites within

Table 1

Paleomagnetic results, declination (Dec), and inclination (Inc), from the Nipissing Diabases, the Matachewan dyke swarm (a), and the Upper Huronian Cobalt Group (b) reported in previous studies

Component	Coordinates	Dec	Inc	α_{95}	κ	R	N	$T_{\text{unblocking}}$
<i>(a) Nipissing Sills, Site A, Gowganda, Canada</i>								
N1	Geographic	24.4	−52.0	4.1	354.0	5.0	5	~580 (°C)
Source: Buchan [27]								
<i>Nipissing Diabase, Englehart, Ontario, Canada</i>								
N3	Geographic	341.2	−59.0	6.0	42.0	47.9	49	~500–580 (°C)
Source: Buchan et al. [28]								
<i>Matachewan Dike Swarm, Kirkland Lake, Canada</i>								
M	Geographic	209.5	−14.8	6.0	39.0	84.8	87	~580 (°C)
Source: Buchan et al. [13]								
<i>(b) Lorrain Formation, “purple siltstone” member at Desbarat, Ontario</i>								
D ^a	Geographic	335.8	−26.1	2.5	114.0	28.8	29	~580 (°C)
	Stratigraphic	340.0	−27.6	4.2	41.0	28.3		
C	Geographic	239.6	61.1	4.3	57.6	19.7	20	~650 (°C)
	Stratigraphic	248.8	53.7	7.4	20.2	19.1		
B	Geographic	39.3	64.7	6.1	37.0	15.6	16	~670 (°C)
	Stratigraphic	18.6	59.6	6.1	59.6	15.7		
A	Geographic	6.6	9.8	5.8	9.0	66.8	75	~690 (°C)
	Stratigraphic	5.4	5.5	5.9	8.7	66.5		
<i>Gowganda Formation Firstbrook Member; Cobalt and Latchford, Ontario</i>								
C ^a	Geographic	99.9	85.4	4.4	38.0	28.3	29	~500 (°C)
	Stratigraphic	51.4	83.3	5.9	21.6	27.7		
B ^a	Geographic	278.3	−55.3	6.0	36.6	16.6	17	~680 (°C)
	Stratigraphic	283.3	−68.6	9.5	15.0	15.9		
A ^a	Geographic	334.1	63.0	4.4	47.8	49.0	50	~680 (°C)
	Stratigraphic	339.1	60.7	4.7	19.3	47.5		
<i>Coleman Member, “gray argillite diamictite”</i>								
B ^a	Geographic	348.6	71.6	5.8	31.3	20.4	21	~300 (°C)
	Stratigraphic	318.9	41.1	22.5	3.0	14.3		
A ^b	Geographic	153.1	70.4	21.2	2.9	18.7	28	~650 (°C)
	Stratigraphic	271.9	69.6	8.5	13.0	25.9		
<i>Coleman Member, “pale red sandstone”</i>								
B ^a	Geographic	348.0	83.9	4.6	16.7	56.5	60	~300 (°C)
	Stratigraphic	6.8	84.1	5.2	13.5	55.6		
A	Geographic	215.9	1.2	6.8	15.8	28.2	30	~690 (°C)
	Stratigraphic	216.3	5.5	6.7	16.3	28.2		
Source: Williams and Schmidt [7]								
<i>Basal Lorrain Formation, Hematitic Breccia near Ville-Marie, Quebec</i>								
B	Geographic	68.7	72.7	2.8	34.1	72.8	75	~580 (°C)
	Stratigraphic	52.1	70.3					
A	Geographic	59.8	4.7	6.7	10.7	42.7	47	~675 (°C)
	Stratigraphic	59.5	2.4					
Source: Schmidt and Williams, 1999 [8]								

the grey-argillitic diamictite and 15 within the red sandstone of the Coleman member (Table 1b). The Coleman-sandstone-A and diamictite-A components had reported unblocking temperatures ranging from 650 °C in the diamictite to 690 °C in the sandstone. The Coleman-B components, steep in direction, failed a regional fold test, whereas the Coleman-diamictite-A, also of high latitude, passed. Williams and Schmidt discarded the Coleman-diamictite-A positive fold test result; previous studies had revealed the Coleman grey beds to be unreliable remanence carriers [28]. Further, the Coleman-diamictite-A component resembles a direction isolated from the 2167-Ma Biscotasing dyke swarm ($D = 267.0^\circ$, $I = 60.5^\circ$) [29], which suggests that the folding event occurred after the intrusion of the Biscotasing. The fold test proved inconclusive for the low-inclination Coleman-sandstone-A direction, which the authors interpreted as an early diagenetic CRM.

Two high-temperature ($T_{\text{unblocking}} = 680^\circ\text{C}$), high-latitude components were isolated from 11 sites in the Firstbrook member (Table 1b). Both Firstbrook-A and Firstbrook-B failed a regional fold test [7]. Williams and Schmidt concluded that the purple argillites within the Firstbrook, like the Coleman grey beds, are unreliable magnetic remanence carriers.

From the 17 sites in the Lorrain “purple siltstone” member, six components were isolated (Lorrain-A, B, C, D, E, and F; Table 1b). Lorrain-B and -C, with unblocking temperatures of 670 °C and 650 °C, respectively, were high-inclination. The Lorrain-E and -F directions have reported unblocking temperatures of 500 °C and 450 °C, respectively. The Lorrain-A and -D, low-inclination, northerly components have unblocking temperatures of 690 °C and 580 °C, respectively. The Lorrain-D was interpreted as being carried by fine-grained (<1 μm) magnetite. A regional fold test proved inconclusive on the Lorrain-A, which Williams and Schmidt concluded to be an early diagenetic CRM. The Lorrain-D exhibited tight

grouping (Fisher’s $\kappa = 114$) but failed a fold test. Fold tests on the Lorrain-B and Lorrain-C component proved inconclusive.

Schmidt and Williams [8] sampled a hematitic breccia of the Lorrain Fm located near Ville-Marie and the Ontario/Quebec border. Two high-temperature components were isolated from the breccia, a westerly, shallow A component, and a westerly, steeply inclined B component (Table 1b). No field tests were performed to constrain the age of acquisition for these components.

Williams and Schmidt [7], and later Schmidt and Williams [8], present a range of evidence to support their low-latitude interpretation for the Gowganda and Lorrain Formations. First, the authors cite “vestiges” of a reversed component within the Lorrain-A and Coleman-sandstone-A, which are not clearly shown in the data and figures provided in the paper [7], to support their interpretation of a post-depositional CRM. The presence of a two-polarity CRM does not place any useful constraints, by itself, on the acquisition time of those secondary components. Second, Williams and Schmidt tentatively interpret the low-inclination Coleman-sandstone-A component as “belonging” to the Lorrain-A direction and thus further evidence for a low paleolatitude. However, the two components fail a McFadden and McElhinny reversal test [31] with very high significance (mean angular difference = 31.2° , p value = 6.35×10^{-12}). The low-inclination, easterly A component, which Schmidt and Williams isolated from the Lorrain hematitic breccia (Table 1), fails common mean direction tests (for two distributions with unequal kappa [32]) with both the Lorrain-A (p value = 5.37×10^{-48}) and Coleman-sandstone-A (p value < 1×10^{-300}). Citing shared unblocking spectra and facies (“Type-A” red bed), Schmidt and Williams explain the 60° clockwise offset between the Lorrain-A and the hematitic breccia A component as a result of post-acquisition fault block rotation. Finally,

Notes to Table 1:

α_{95} = Radius of 95% confidence circle about the Fisher mean direction; κ = Fisher dispersion coefficient (low κ = high dispersion, high κ = low dispersion); N = number of paleomagnetic specimens from which the component was isolated; R = length of the resultant vector sum of all the vectors in the component’s Fisher population and is related to the degree of dispersion; $T_{\text{unblocking}}$ = maximum temperature for which the component is stable/present.

^a Negative fold test at >95% confidence.

^b Positive fold test at >95% confidence.

Williams and Schmidt cite the conglomerate test performed on Buchan et al.'s C component. As noted above, Buchan's test is too weak to place any constraints on the low-inclination Coleman-C direction. Additionally, Buchan's C direction lies closer to Williams and Schmidt's Lorrain-D component, rather than the Lorrain-A. Hence, there is no hard evidence to constrain the acquisition time of the Lorrain-A, Coleman-sandstone-A, or hematitic breccia A components. The claim that the Lorrain-A component was acquired soon after deposition is questionable [7], and further work is required to constrain the paleolatitude of the Gowganda and Lorrain formations.

4. Methods

Our site was located in a road-cut along highway 17 near the town of Desbarats, N 46° 20.538', W 83° 55.926', which is one of the same sites of the "purple siltstone" member of the Lorrain Formation sampled by Williams and Schmidt [7] (Fig. 1). In the northwest section of this exposure, we discovered a ductile chevron fold covering an approximately 50-m² area, with an axis plunging 19° to the WSW. This is roughly perpendicular to the high-temperature characteristic direction reported for this unit [7], making it ideal for a paleomagnetic fold test on the component. The downward dipping part is buried and the upper dipping end was removed during highway construction, leaving a stretch ~10 m long exposed, parallel to the road, and in good condition. (Subsequent to our sampling, the site was blasted by a road construction crew, and we do not know whether any portion of the fold remains in the outcrop.) Normal vectors to the bedding planes on opposite limbs of the fold measure ~60° apart, providing ample structural control for the fold test.

The exact nature of the fold is somewhat uncertain. Analysis of intergranular space (volume percentage of pore, cement, and matrix space) of three thin sections, one from the fold axis and one from each fold limb, indicates that the folding event occurred after cementation of grains within the fold beds, at a maximum depth of ~1 km. Intergranular space within the fold axis (30%) was significantly greater than spacing in the fold limbs (21.5% and 23.5%). Compaction index ranges from 0.34 to 0.4, with slightly less compaction

along the fold axis. There is no distinguishable difference between vertical and horizontal directions in all three samples. These results are consistent with a post-lithification bending event that occurred before significant vertical compaction of the silty sandstone fold beds. Further, the fold geometry, a chevron crease continuing for several meters, suggests that the meter-scale-thick silty sandstone units had lithified enough to focus deformation at bedding plane clay units. We found no evidence of soft-sediment deformation upon fine-scale examination of the fold block or during sample preparation.

Using a portable water-cooled diamond-bladed concrete saw, we sliced out and oriented a boomerang-shaped block sample, 45 cm long, ~10 cm wide, and ~3 cm thick, which spans the crest of the chevron fold of the Lorrain purple siltstone described above (Fig. 2). A total of 14 cores, Lorrain "purple siltstone" at Desbarats (LSD), were drilled at ~30 cm intervals spaced stratigraphically through the road-cut exposure on the south side of the highway, overlapping holes drilled by Williams and Schmidt. These samples were oriented in situ using both magnetic and solar compasses. The mean magnetic declination was measured at 8°1.2'W, in rough agreement with the value of 7°33'W predicted by the IGRF model for the site.

In order to get the highest sampling density of material from the boomerang block, cores ~2.5 cm in diameter were drilled in the laboratory from two symmetrical limbs, "A" and "B," of the fold (Fig. 2) using standard techniques. Cores were drilled as closely packed as possible and farthest from the center of the fold (where the orientation of the bedding begins to curve about the fold axis). The orientation of the bedding planes for a few samples near the fold axis was modeled, assuming the curve of the bedding to be a circle arc. Cores were then extracted from the rock and sliced perpendicular to their central axis into pieces 0.5–2 cm in length. In total, 118 Lorrain fold test (LFT) samples were removed from the boomerang fold block for study. Thermomagnetic and coercivity determinations were run in dry He gas on representative lithological samples on the MicroMag[®] system at Tokyo University.

NRM measurements were made with a 2G Enterprises[™] DC SQUID magnetometer with on-line,

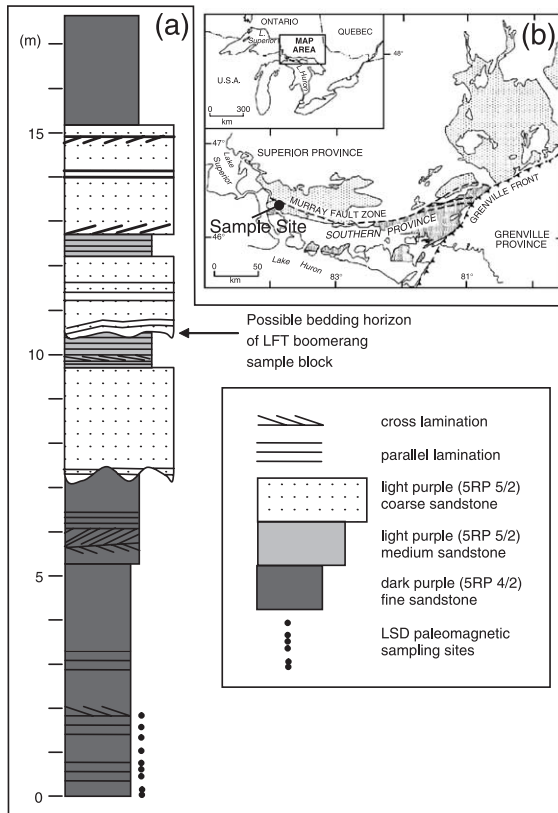


Fig. 1. Stratigraphy (a) of Lorrain “purple siltstone” member exposure along Highway 17, near Desbarats, Ontario, with stratigraphic positions of the LSD and LFT samples indicated. Regional geologic map (b) of the extent of the Huronian Supergroup (adapted from [7]). Light stipple indicates areas of lower metamorphic grade; dense stippling indicates areas of higher metamorphic grade.

computer-controlled alternating field (AF) demagnetization coils using an automated, vacuum pick-and-put sample changing array [33]. AF demagnetization was run in 2 mT steps up to 10 mT to remove viscous components and any random field components gained during transport from Desbarats, Canada, to Caltech, and sample preparation. Subsequently, samples from the fold test boomerang (LFT) were run using standard techniques in a magnetically shielded ASC™ oven with $\pm 10^\circ \text{C}$ error in two groups. The first group of 74 samples was demagnetized at 150, 250, 350, 425, 500, 550, and 575, and in 10° steps up to 670°C , in air. The second group of 44 samples was demagnetized at 150, 250, 350, 450, 525, and 550, in 10°C steps up to 590° , and then in 10° steps from 595 to 685°C , in nitrogen. Directions of both

sets became random above $660\text{--}670^\circ \text{C}$, at which point the samples were judged to be completely demagnetized. Thirty-six LSD samples were run in thermal steps of 150, 250, 350, 450, 500, 525, and 550, in 10°C steps up to 640°C , and then in 5°C steps up to 680°C . LSD samples appeared to be completely demagnetized around $660\text{--}670^\circ \text{C}$. Complete up and down measurements were done for statistical robustness, and those with errors $\geq 10^\circ$ were redone by hand. Principal magnetic components were found using the least squares methods of Kirschvink [34], with critical threshold (MAD) values for lines and planes of $\sim 10^\circ$ and 15° , respectively. Raw demagnetization data for the LSD

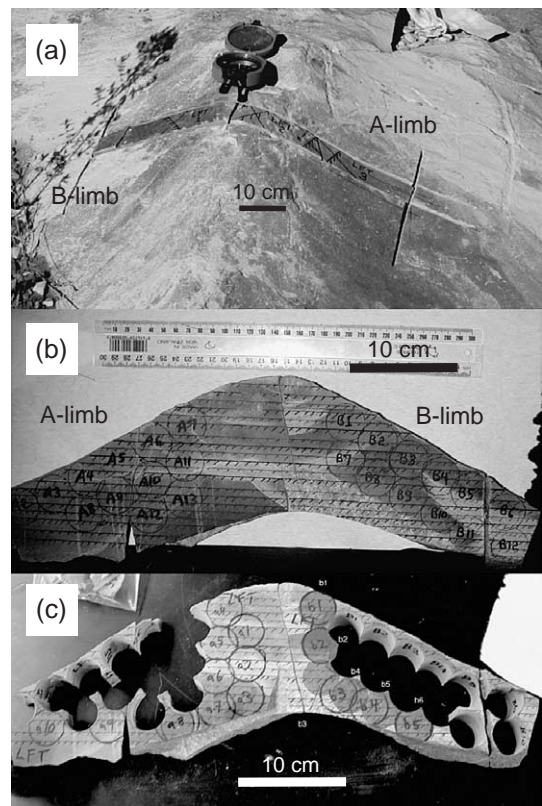


Fig. 2. Lorrain fold test (LFT) boomerang sample block: (a) in place in the field, (b) before extraction of the first group of 74 specimens, and (c) before extraction of the second group of 44 specimens. Note that cores extracted from B-limb in (c) are as indicated by faint grey circles and white lettering. The parallel black lines on the flat face provided accurate ($< 1^\circ$) relative orientations between specimens; the entire block was constrained by three independent block sample orientation marks.

and LFT samples, along with a list and description of our least squares interpretations will be deposited in the MagIC database as soon as it becomes operational. Until then, data can be accessed as compressed .zip files linked to the Caltech paleomagnetism lab homepage (http://www.caltech.edu/Maglab/Huronian2002_Data.zip).

5. Rock magnetic and paleomagnetic results

Based on the status of the “purple siltstone” member as one of the earliest red beds in Earth history and on the past paleomagnetic work [7], our initial presumption was that the magnetic mineralogy in the “purple siltstone” member of the Lorrain Formation would be dominated by stable, medium- to fine-grained hematite. Fig. 3a shows the results of a typical thermomagnetic experiment on a matrix sample of the boomerang block, run in a field of 398 kA/m (5 kG). The heating and cooling curves are irreversible, with the sample moment increasing by nearly a factor of 5 during the cooling leg. No evidence of magnetite dominated Curie temperatures is seen on heating between ~ 550 – 580 °C, whereas this is prominent upon cooling. Hysteresis loops (Fig. 3b) also change drastically after heating, with the initial data suggesting domination by high-coercivity anti-ferromagnetic and paramagnetic materials. After heating, the loops resemble those produced by single-domain dispersion of ferrimagnetic materials like magnetite or maghemite. These results resemble those typical of oxidized banded iron formations (BIFs), in which fine-grained ferric oxide pigments may revert to magnetite upon heating in non-oxic conditions [35].

Thermal demagnetization of the LSD samples yielded four components (Table 2a, Fig. 4): LSD-D, a high inclination, northwesterly component that corresponds approximately with the present local field direction (Fig. 5b); LSD-C, a west to southwesterly, medium-inclination, low-temperature component (maximum unblocking temperature of ~ 450 °C) (Fig. 5a); LSD-B, a low-inclination, intermediate-temperature (450–550 °C) component that is similar in blocking temperature spectra and high κ to the Lorrain-D component (Fig. 5c); and LSD-A, an especially stable intermediate- to high-temperature

component that is nearly identical to the Lorrain-A component of Williams and Schmidt (Fig. 6). The LSD-A component has a low κ ($\kappa = 12.49$, $N = 35$) but exhibits stability; it forms clumps in the orthographic and equal area projection at temperatures starting as low as 550 °C and until its maximum unblocking temperature of 660 °C (mean = 660°).

Demagnetization of the LFT samples reveals the prevalence of a low-inclination northerly component, LFT-A, isolated by high-temperature thermal demagnetization and resolved by least squares line and plane analysis. LFT-A has similar dispersion ($\kappa = 7.13$), clumping behavior in the orthographic and equal area projection and unblocking spectra (for the first 74 specimens, $T_{\text{unblocking}} = 610$ – 670 °C,

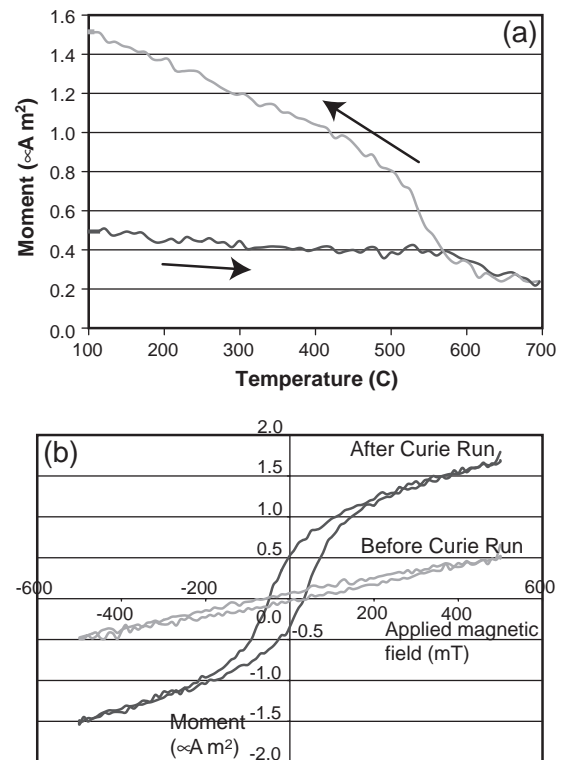


Fig. 3. Thermomagnetic and hysteretic properties of the purple siltstone lithology of the Lorrain formation. The Curie temperature run shown in (a) reveals that a fine-grained ferromagnetic phase (like magnetite) forms upon heating the samples above ~ 600 °C, yielding a strong magnetization upon cooling. Similarly, the hysteresis loops shown in (b) reveals a switch from a typical anti-ferromagnetic pattern like that expected for fine-grained hematite to a more ferrimagnetic pattern after heating.

Table 2

Paleomagnetic results from (a) stratigraphic sampling of the Lorrain “purple siltstone” member at Desbarats (LSD), and (b) the Lorrain “purple siltstone” member, boomerang fold block (LFT)

(a) Paleomagnetic results from stratigraphic sampling of the Lorrain “purple siltstone” at Desbarat (LSD)									
Component		Dec	Inc	α_{95}	κ	R	N	$T_{\text{unblocking}}$	
D	Geographic	328.6	67.5	6.32	15.68	32.83	35	~150–250 (°C)	
	Stratigraphic	311.4	58.4	6.51	14.86	32.71			
C	Geographic	249.6	39.9	2.69	82.43	34.59	35	~450 (°C)	
	Stratigraphic	253.1	28.5	2.73	80.06	34.58			
B	Geographic	332.0	−25.7	3.38	52.41	34.35	35	~550–580 (°C)	
	Stratigraphic	337.9	−32.1	3.43	50.94	34.33			
A	Geographic	10.3	0.3	7.15	12.49	32.28	35	~660–670 (°C)	
	Stratigraphic	10.2	1.4	7.13	12.54	32.29			

(b) Paleomagnetic results from the boomerang fold block, Lorrain fold test (LFT), “purple siltstone” member, Desbarat									
Component	Fold limb		Dec	Inc	α_{95}	κ	R	N	$T_{\text{unblocking}}$
D	Both	Geographic	315.6	75.1	3.01	27.99	79.11	82	~150–250 (°C)
		Stratigraphic	277.5	59.0	5.54	8.96	72.96		
	A-limb	In situ	318.9	73.2	3.57	41.00	39.05	40	
		Tilt-corrected	229.6	67.5	4.35	28.00	38.61		
C	B-limb	In situ	311.6	76.9	4.84	21.69	40.11	42	
		Tilt-corrected	299.2	42.1	4.84	21.69	40.11		
	p value	6.8129×10^{-62}	Confidence level: 100%						
C	Both	Geographic	273.5	59.4	2.89	23.86	100.16	104.5	~450 (°C)
		Stratigraphic	258.3	38.0	5.22	8.01	91.58		
	A-limb	In situ	268.4	64.3	3.76	24.72	57.61	60	
		Tilt-corrected	233.3	47.7	4.25	19.61	56.99		
	B-limb	In situ	278.4	52.5	3.80	32.62	43.17	44.5	
		Tilt-corrected	281.7	19.1	3.80	32.64	43.17		
p value	1.02639×10^{-95}	Confidence level: 100%							
B	Both	Geographic	342.3	−29.3	2.17	37.46	112.93	116	~550–580 (°C)
		Stratigraphic	354.0	−23.0	4.98	7.93	101.50		
	A-limb	In situ	340.2	−27.9	3.12	32.81	63.05	65	
		Tilt-corrected	347.8	−1.3	3.41	27.58	62.68		
	B-limb	In situ	345.1	−31.0	2.85	50.01	50.00	51	
		Tilt-corrected	6.3	−50.1	3.19	40.15	49.75		
p value	3.425×10^{-159}	Confidence level: 100%							
A	Both	Geographic	11.7	−32.3	6.29	7.13	71.07	82.5	~660–670 (°C)
		Stratigraphic	20.0	−16.1	7.16	5.73	68.28		
	A-limb	In situ	5.8	−33.5	8.33	7.35	39.88	46	
		Tilt-corrected	10.5	−4.7	8.46	7.17	39.72		
	B-limb	In situ	18.9	−30.1	9.54	7.17	31.55	36.5	
		Tilt-corrected	34.3	−30.2	9.51	7.21	31.58		
p value	6.9971×10^{-13}	Confidence level: ~100%							

In (b), component directions are reported for specimens from the two limbs of the boomerang, individually (A-limb, B-limb) and together (Both). All four components failed a McFadden fold test [36] with extremely high significance, in which tilt-corrected directions from the “A” and “B” limbs of the boomerang were compared using a common mean direction test for two Fisher populations with unequal κ [32]. p values indicate the probability that the two tilt-corrected directions are identical (a positive fold test). p values for all four components isolated from the LFT specimens are $\ll 0.05$ and therefore indicate highly negative fold tests. Symbols are as in Table 1.

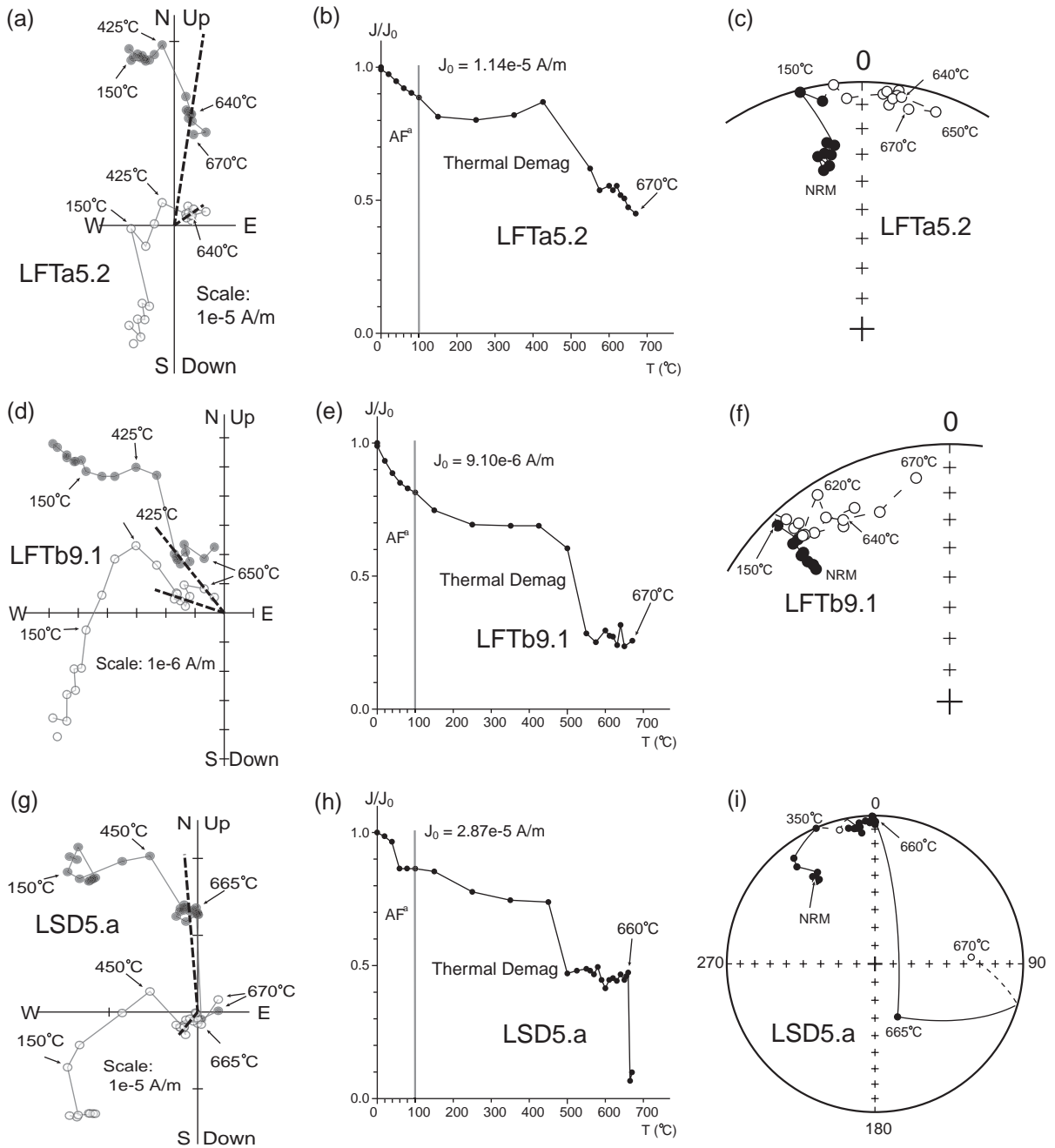


Fig. 4. Paleomagnetic results from four samples LFTa5.2, LFTb9.1, and LSD5.a presented in geographic coordinates. Orthogonal projections in (a), (d), and (g) show the sample magnetic moment's intensity for each AF and thermal demagnetization step, projected on the E/N vertical plane (open circles) and horizontal plane (closed circles). Equal-area, orthographic projections (c), (f), and (i) show sample moment's direction for each demag step. J/J_0 plots (b), (e), and (h) show the moment magnitude/intensity for each demag step with respect to the initial remanence moment, J_0 (NRM). Demagnetization steps of interest are labeled on each diagram. AF^a steps indicated on J/J_0 plots were run at 2, 4, 6, 8, and 10 mT.

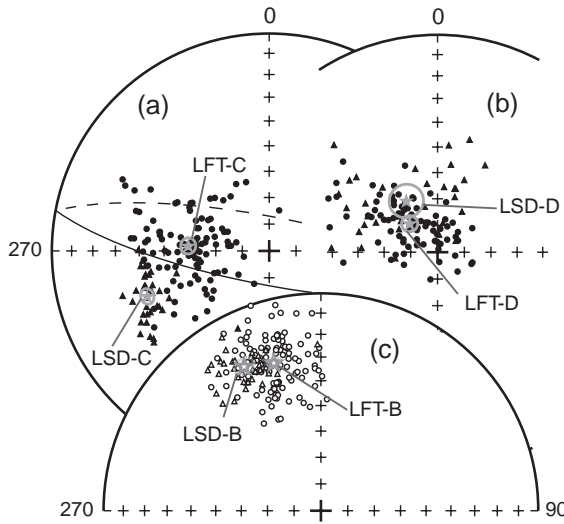


Fig. 5. Orthographic, equal projections comparing the in situ -B (c), -C (a), and -D (b) components isolated from the LFT (circles) and LSD (triangles) sample specimens. Stars indicate Fisher mean directions with circles of 95% confidence (radius = $\alpha-95$). Great circles indicate circle fits used to isolate directions in specimens. Closed symbols and solid lines represent directions in the Northern Hemisphere, while open symbols and dashed lines indicate directions in the Southern Hemisphere.

mean = 638 ± 17 °C; for the second 44 specimens, $T_{\text{unblocking}} = 655\text{--}670$ °C, mean = 658 ± 6 °C) to the LSD-A direction (Fig. 6). Mean unblocking temperatures were determined by averaging together the individual LFT-A maximum unblocking temperature for each specimen in which the component could be found. For both means, error was calculated as the standard root mean squared. However, the in situ LFT-A direction is separated by 32.6° from the LSD-A direction. The tilt-corrected LFT-A directions for samples from the A- and B-limbs of the boomerang fold block are separated by 34.0° and were compared using the McFadden common mean direction fold test [36]. The LFT-A direction failed a Class-C fold test with extremely high significance (p value = 4.98×10^{-9}), and must therefore post-date the deformation (Table 2b, Fig. 7). Pre-folding A- and B-limb directions disagree by 11.6° ; however, the two directions pass a Class-C McFadden and McElhinny common mean direction test [31] with 95% confidence (p value = 0.075). Upon unfolding, specimen directions from each limb diverge in nearly orthogonal directions and the combined kappa is not

increased by either folding or unfolding along the fold axis. Therefore, we exclude the possibility of a pre-folding or synfold acquisition for the LFT-A component.

The LFT samples yielded three low- to intermediate-temperature components, termed LFT-B, -C, and -D. All three of these failed the McFadden fold test with p values smaller than 10^{-60} (Table 2b). The LFT-B component has a shallow NNE direction and a maximum unblocking temperature around 580 °C, suggesting magnetite or maghemite as the carrier (Fig. 5c). Like the LSD-B and Lorrain-D components, the LFT-B has low dispersion and unblocking spectra between ~ 450 and 580 °C. However, the direction is distinct from the other two components. The LFT-C and -D share identical unblocking temperature spectra with the corresponding LSD-C and -D directions.

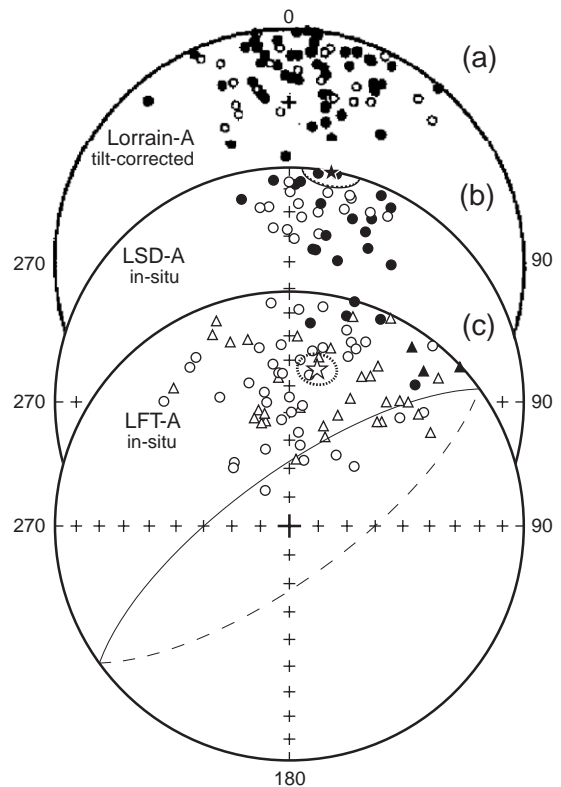


Fig. 6. Equal-area projections comparing Williams and Schmidt's [7] Lorrain-A components (a), with the LSD-A (b) and LFT-A (c) components isolated in this study. Symbols are as in Fig. 5. Circles and triangles in (c) indicate directions from the "A" and "B" limbs, respectively, of the LFT boomerang sample block.

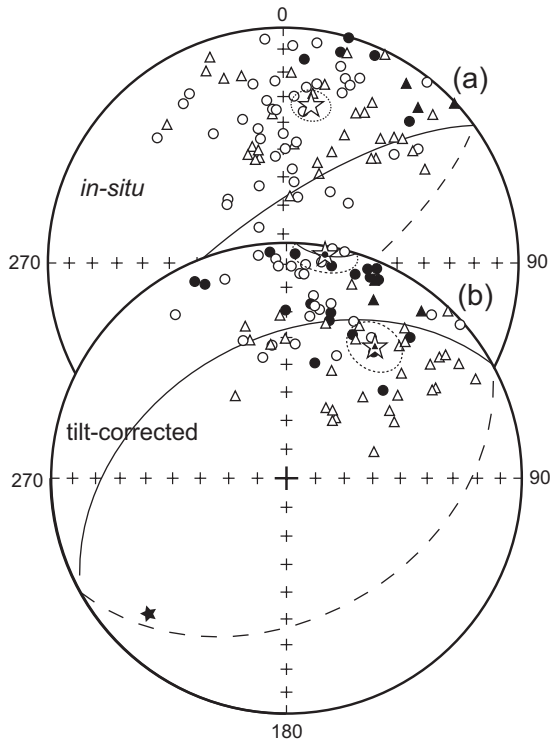


Fig. 7. Negative fold test on the LFT-A direction, in situ (a) and tilt-corrected (b). Stars indicate Fisher means with circles of 95% confidence. Symbols are as in Fig. 5. Circles and triangles in (b) indicate directions from the “A” and “B” limbs, of the LFT boomerang sample block. Stars with a circle or triangle inside indicate the Fisher mean with circle of 95% confidence for the “A” and “B” limb specimens, respectively. The black star in the lower quadrant of (b) indicates the fold axis of the LFT boomerang block.

However, both the LFT-C (Fig. 5a) and -D (Fig. 5b) are separated from the LSD-C and -D directions by 24.6° and 8.6° , respectively.

6. Discussion

The fold test shows with extremely high significance that none of the Desbarats directions isolated from the boomerang fold block are primary. In terms of their blocking temperature ranges, the various components identified in our study match well with those reported by Williams and Schmidt [7], so it is unlikely that their Lorrain-A component can be used to constrain the paleolatitude of Lorrain or underlying Gowganda formations. However, the in situ

LFT-B, -C, and -D components are separated from the corresponding LSD-B, -C, and -D components by 9.8° , 24.6° , and 8.6° , respectively, and the LFT-A direction is separated by 43.4° from the Williams and Schmidt Lorrain-A direction and by 32.6° from our LSD-A direction. We present three arguments to explain these directional differences and defend our identification of the LFT-A component with the LSD-A and Lorrain-A: post-acquisition tilting of the LFT outcrop with respect to the LSD outcrop, heterogeneous acquisition of components during post-depositional metamorphic and diagenetic processes, and/or secular variation during chemical remanence acquisition.

The LSD-D and LFT-D components most likely correspond to a present local field direction (Fig. 5b). Motion with AF demagnetization from 2 to 10 mT to the first thermal step was fit to produce both the LSD-D and LFT-D components, recording the removal of a soft-viscous remanent magnetization. While the mean directions for both disagree by 8.6° and the directions fail a Class-B McFadden and McElhinny common mean direction test [31] with 97% confidence, they are high-inclination and the LSD-D mean has high dispersion (low κ). The in situ and tilt-corrected LSD-C and LFT-C paleopoles disagree by 24.6° (Table 3). However, the two components share the same unblocking spectra and have similar behavior in the orthographic projection. The LFT-C pole overlaps a pole for the Biscotasing dyke swarm (2167 ± 2 Ma) reported by Buchan et al. [29] on the Superior Province apparent polar wander (APW) path. This suggests that the LFT-C component may date to the time of the Biscotasing dyke swarm at ~ 2167 Ma. The LSD-C paleopole does not lie on Proterozoic Superior Province APW. Therefore, either the LSD-C and LFT-C components were acquired at widely different times, or the correspondence of the LFT-C pole to the Biscotasing pole is a coincidence and the -C components are of younger age. The unblocking temperature spectra of the -C components, 150 – 450°C , suggest titanium-rich titanomagnetite or magnetite as possible magnetic carriers.

Both the LSD-B and LFT-B directions have very tight grouping, similar to the Williams and Schmidt [7] Lorrain-D direction (Fig. 5). All three have very high κ , suggesting that they may be due to a secondary thermal remanent magnetization (TRM).

Table 3

Important paleopoles on the Superior Province APW path, ~2.47 to ~1.6 Ga; d_p and d_m are the semi-axes of the oval of 95% confidence about the mean paleopole; for the last four poles, α_{95} = radius of the circle of 95% confidence about the mean paleopole

Component	Pole Dec	Pole Inc	d_p	d_m	Source
LFT-A ^a	265.1	−25.2	3.9	6.9	This study
LSD-A	261.9	−42.9	3.6	7.2	This study
Lorrain-A	266.2	48.1	3	5.9	[7]
LFT-B	295.1	−26	1.3	2.4	This study
LSD-B	306.3	−25	2	3.6	This study
Lorrain-D	302.4	−26	1.4	2.7	[7]
LFT-C ^b	34.5	−30	3.3	4.3	This study
LSD-C ^b	36.1	−3.3	1.9	3.2	This study
LFT-C	214.5	30	3.3	4.3	This study
LSD-C	216.1	3.3	1.9	3.2	This study
Bicostasing ^{c,d}	223.3	27.8	9.4	12.3	[29]
Fort Frances ^{c,d}	184	43	5	7	[30]
Marathon-N ^c	195.8	42.7	6.7	9.2	[45]
Marathon-R ^d	174.7	49	6	9	[45]
Molson-C1 ^{c,d}	180	53	7.6	9.7	[47]
Molson-C2 ^{c,d}	216	28.7	7.3	9.1	[47]
Nipissing N1 ^{c,d}	260	−14	4	6	[30]
Nipissing N3	341.2	29.5	6.6	8.9	[28]
Senneterre ^d	284.3	−15.3	4.4	7	[29]

Component	Pole Dec	Pole Inc	α_{95}	Source
Matachewan-N ^{c,d}	66	50	14	[46]
Matachewan-R ^{c,d}	58	40	4	[46]
Molson-A	263.5	15.4	4.1	[48]
Molson-B ^{c,d}	219.2	27.1	3.8	[48]

^a Probable VGP.

^b Anti-parallel component (reflected through origin) for comparison.

^c Pole position verified by paleomagnetic field stability test.

^d Paleopole well dated.

Paleopoles (in situ) for the three components lie within ~5–10° of each other, which is consistent with this interpretation (Table 3, Fig. 8). The in situ LFT-B and LSD-B and the in situ LFT-B and Lorrain-D directions are statistically distinct (p value = 9.12×10^{-9} for a common mean direction test between two Fisher populations with unequal κ [32] between LFT-B and LSD-B, p value = 5×10^{-6} for LFT-B vs. Lorrain-D). However, the LSD-B and Lorrain-D pass a 95% confidence, Class-A McFadden and McElhinny common mean direction test [31]. The tilt-corrected poles for these three do not appear to match any paleopole on the Paleoproterozoic APW path for the Superior Province. The three in situ paleopoles do correspond with a pole

proposed for a secondary direction isolated from 36 sites in the Dollyberry Lake Volcanics at the base of the Huronian Supergroup by Stupavsky and Symons [37], who asserted that the component was most likely acquired at $\sim 1900 \pm 100$ Ma. McLennan et al. [38] found evidence for post-depositional alteration of the Upper Huronian sedimentary sequence (specifically the Gowganda and Gordon Lake formations) at 1667 ± 120 Ma. Therefore, the three paleopoles may fit on a post-1750 Ma Mesoproterozoic segment of the Superior Province APW at ~ 1667 Ma. Further, this suggests that the outcrop has seen minimal tectonic offset since the acquisition of the LSD-B component.

Although the in situ LSD-A direction is separated from the Williams and Schmidt [7] Lorrain-A by only 10.2° (common mean direction test [32], p value = 0.022), the in situ LSD-A and LFT-A directions are separated by 32.6° and are statistically distinguishable (common mean direction test [32], p value = 2.00×10^{-16}). The LFT-A component fails both common mean direction and reversal tests with greater than 95% confidence with all six in situ Williams and Schmidt components and all four in situ LSD components (Table 4). Compared with each of the LSD components, the LFT-A correlates best with the LSD-A direction (followed by the LSD-B direction), and a test between the LFT-A and LFT-B directions yields a lower p value than the LSD-A/LFT-A test. Therefore, among the LSD components, we identify the LFT-A direction with LSD-A. The LFT boomerang block was extracted from the lighter hued beds (~5RP 5/2) north of Highway 17, within 50 m of the LSD locality. These beds stratigraphically overlie the darker (~5RP 4/2) beds from which the LSD samples were removed on the southeast side of the Highway 17 road cut exposure. Due to the presence of the road, it is not possible to map the site for local tectonic effects, but the presence of significant variation in the bedding attitudes between the LSD and LFT sites argues that bedding deformation may be at fault for the angular difference between the LFT-A and LSD-A components. The strata of the Desbarats outcrop are gently folded. Based upon bedding angles in the southern-side outcrop along Highway 17, a tilt-angle difference of as large as 15° is possible within the outcrop. In addition to the 19° westerly plunge of the chevron fold, the normal

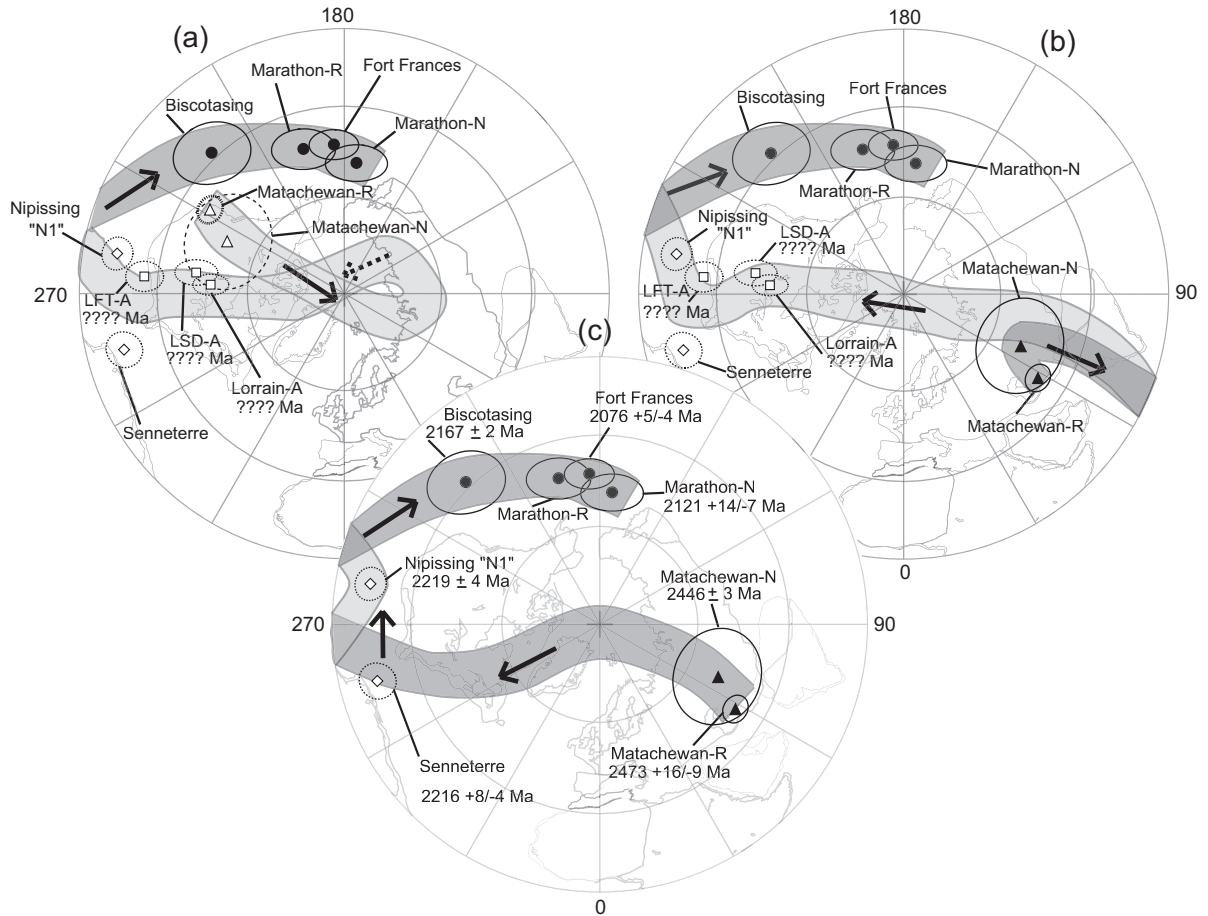


Fig. 8. Possible APW paths for the Huronian Supergroup (and Superior Province) for ~ 2.5 – 2.1 Ga (a–c). APW paths (a), (b), and (c) have been constructed to allow the Huronian Basin to move to latitudes above 33° (the critical latitude line for an ice albedo runaway) between ~ 2.45 and 2.2 Ga. While highly speculative, each of the APW pathways is possible given the lack of adequate constraints on the age of acquisition for the LFT-A, LSD-A, and Lorrain-A components. Positions for the Biscotasing and Senneterre paleopoles are from Buchan et al. [29], for the Nipissing “N1” and Fort Frances poles are from Buchan et al. [30], for the Marathon-R (reverse) and Marathon-N (normal) poles are from Buchan et al. [45], for the Matachewan-R and Matachewan-N are from Bates and Halls [46], for the Lorrain-A and Lorrain-D poles are from Williams and Schmidt [7], and for the LFT-A, LSD-A, LFT-B, and LSD-B poles are from this study. Ages for the Biscotasing, Senneterre poles are from [29], for the Fort Frances and Marathon-N poles are from [45], for the Nipissing “N1” pole are from Corfu and Andrews [17], and for the Matachewan-R and Matachewan-N poles are from Heaman [16]. The LFT paleopole may be a VGP.

vectors to the bedding planes between the LSD site and the fold block A-limb are nearly 40° apart, and between LSD and B-limb, they differ by 25° . Hence, the observed divergence could be of later tectonic origin.

Disagreement between the LFT-A, LSD-A, and Lorrain-A directions may also be a result of secular variation. Regional variance in the post-depositional acquisition of the LFT-A component and the stratigraphic thickness of the boomerang fold-block (<10

cm) allows for the LFT-A to be a virtual geomagnetic pole (VGP) of the LSD-A and Lorrain-A directions. Based upon the reported Lorrain-A κ value, the calculated θ_{95} value for the component is 48° , which is greater than the component’s angular separation from the LFT-A direction (Table 4). Hence, we cannot exclude the VGP hypothesis with 95% confidence.

The thermal demagnetization of the Lorrain-A, LSD-A, and LFT-A components provides the strongest

Table 4

Results of common mean direction tests for two Fisher distributions with unequal kappa, between the LFT-A component and several other relevant components (Lorrain and Coleman components are from Williams and Schmidt [7], and Nipissing “N1” and “N3” components are from Buchan [27] and Buchan et al. [28])

ID	Coordinates	Angular separation	θ_{95}^a	Result (95% confidence)	p value ^b
LFT-A	In situ	–	52.43	–	–
Lorrain-A	In situ	43.4	46.67	Fails	5.19×10^{-34}
Lorrain-B ^c	Tilt-corrected	87.9	18.13	Fails	3.24×10^{-158}
Lorrain-B ^c	In situ	85.3	23.02	Fails	1.30×10^{-124}
Lorrain-C ^c	In situ	42.1	18.45	Fails	3.73×10^{-41}
Lorrain-D	In situ	31.8	13.11	Fails	1.41×10^{-29}
Lorrain-E	In situ	86.8	25.43	Fails	2.53×10^{-108}
Lorrain-F ^c	In situ	46.9	21.92	Fails	2.68×10^{-59}
LSD-A	In situ	32.6	39.61	Fails	2.00×10^{-16}
LSD-B	In situ	35.1	19.34	Fails	1.57×10^{-32}
LSD-C ^c	In situ	46.6	23.84	Fails	1.74×10^{-51}
LSD-D	In situ	104.92	35.36	Fails	4.85×10^{-174}
LFT-B	In situ	25.35	22.87	Fails	9.69×10^{-20}
Nipissing “N1” Site B	NA	14.3	15.10	Fails ^d	7.44×10^{-4}
Nipissing “N1” Site A	NA	21.8	7.44	Fails ^d	5.47×10^{-13}
Nipissing “N3”	NA	69.2	–	Fails	1.09×10^{-120}

^a Butler [44], p. 106.

^b Lower p values correspond to greater level of confidence with which the null hypothesis that the two components are parallel can be rejected (Fisher et al. [32], pp. 210–211).

^c Antipodal direction used.

^d Passes common mean direction test with equal kappa (McFadden and McElhinny [31]). However, result is indeterminate as the critical angle exceeds 20°. Both tests may be biased by the small number of specimens in which the “N1” site directions were isolated.

argument for common identification of the LFT-A, LSD-A, and Lorrain-A components, as well as the LFT-B, LSD-B, and Lorrain-D components. Williams and Schmidt’s Lorrain-A and -D scatter cones overlap in the equal-area projection. They separated the two populations largely based upon their unblocking temperature spectra [7]. Likewise, the LFT/LSD-A and -B components interfinger. Both -B directions were isolated from movement between 425 °C and 580 °C. In each sample from which both the LFT/LSD-A and the LFT/LSD-B directions were found, the -B direction moved from ~425 °C to a high-temperature cluster that remained stable between ~580° and 660–680 °C. Our LFT/LSD-A directions were fit by anchoring these high-temperature, high-stability clusters to the origin. In every case in which a discernable cluster was present, the cluster/origin fit was distinguishable in direction from the -B direction fit for that specimen. This behavior, shared by both LFT and LSD specimens, strongly suggests that the two components share a common genesis. LFT and LSD specimen J/J_0 plots (Fig. 4) show a decrease in the sample intensities from 450° to 580°, consistent with titanomagnetite or

maghemite as the magnetic carriers. Similarly, the Lorrain-D component was isolated within this temperature range, and Williams and Schmidt suggest magnetite as the probable remanence carrier for their Lorrain-D component [7]. The overlapping Lorrain-A and -D scatter cones and the shared Lorrain-A, LFT-A, LSD-A, and Lorrain-D, LFT-B, LSD-B unblocking spectra, respectively, again suggest common genesis for the components.

Sample demagnetization behavior suggests that the LFT and LSD-A components were acquired as CRM. For the LFT and LSD-A components, some specimens from the same cores, drilled parallel to the paleobedding, gave completely different A directions. It is unlikely that a secondary TRM could produce this small scale difference in directions. The high dispersion of the -A components, and the negative fold test on the LFT-A, further suggest that the directions are CRMs acquired sometime after the folding event in the “purple siltstone member” of the Lorrain, probably a result of secondary oxidization. Williams and Schmidt’s interpretation of the Lorrain-A as a CRM strengthens our argument for common genesis

of the LFT-A, LSD-A, and Lorrain-A components. (However, if this is true, the Lorrain-A CRM cannot be early diagenetic as they imply [7].)

An alternative to our interpretation is suggested by common mean direction tests between the LFT-A components and Buchan et al.'s Nipissing "N1" directions (Table 4). In terms of angular difference and p value, the LFT-A component lies closest to Sites A and B, Nipissing "N1" directions [27]. McFadden and McElhinny' common direction test for LFT-A vs. the two "N1" components yields positive, but inconclusive, results (critical angle of 95% confidence greater than 20°). This suggests that the high p values for both tests between the LFT-A and Nipissing directions may be an artificial result, caused by the low number of specimens in the Nipissing Fisher populations. However, a pole calculated for the LFT-A direction lies between the LSD-A and Lorrain-A poles and the Nipissing "N1" paleopole. Surface exposures of ~100 m thick Nipissing diabase have been mapped 1 km to the north, 0.7 km to the east, and 1.2 km to the southeast of our LFT and LSD sampling sites [39]. This raises two possibilities: that the LFT-A direction is contaminated with a Nipissing "N1" overprint, or that the LFT-A direction was acquired sometime after the LSD-A and Lorrain-A components, requiring the Nipissing diabase intrusion of the Huronian Supergroup to post-date all three components. The former seems highly unlikely. The LFT and LSD sample localities are located approximately 50 m apart. A regional thermal overprint would contaminate directions isolated from both sites. Local subsurface intrusion of the Nipissing could allow for contamination of the LFT-A direction without affecting the LSD-A component, although even this can be ruled out as unlikely through comparison of the LFT-A and LSD-A demagnetization behavior. Further, no evidence of small scale intrusion was detected at the LFT outcrop. The latter possibility is more likely and cannot be ruled out. A baked-contact test between the Nipissing diabase and the Lorrain "purple siltstone" member would be ideal for determining the relative timing of the Lorrain low-inclination components and Nipissing "N1" directions.

Despite numerous attempts at isotope dating and attempted correlations of stable isotope signatures between the Huronian, and Paleoproterozoic units in South Africa, Siberia, and Australia, the time of

deposition for all four Upper Huronian sedimentary formations is constrained loosely between ~2.4 and ~2.3 Ga. Even if the low-inclination LFT-A, LSD-A, and Lorrain-A were acquired prior to the ~2.2 Ga intrusion of the Nipissing sills, this could allow up to ~200 Ma for the Huronian basin to transit from the low Matachewan paleolatitude to high latitude and back at least once (Fig. 8).

7. Conclusion

"Extraordinary claims require extraordinary proof" (atr. Carl Sagan). The negative field test from the LFT chevron fold shows that the Huronian paleomagnetic data are not in the class of extraordinary results needed to invoke the specter of low-latitude glaciation. The low-inclination component may be a CRM acquired sometime after post-depositional deformation of the LFT outcrop. Therefore, the paleolatitude of the Lorrain and underlying Gowganda formations are uncertain. Given that the magnetization carried by hematite is secondary and may be a CRM resulting from post-depositional oxidation, the interpretation of the "purple siltstone" member as an early indicator of atmospheric oxygen is also weakened. The secondary oxidization event may, however, be a record of rising levels of oxygen in the Paleoproterozoic atmosphere, even after the Makganyene event. Therefore, further field stability tests on the remanent magnetizations of the Lorrain Formation, the underlying Gowganda, and the overlying Gordon Lake and Bar River formations are required to constrain the paleolatitudes and the APW for the upper Huronian sedimentary sequence and the rise of atmospheric oxygen in the Paleoproterozoic.

Numerous correlations have been attempted between the exposures of Paleoproterozoic glacial units in both Canada and South Africa, as low-latitude events should be globally synchronous. However, as the Huronian paleolatitudes are truly unknown, this is no longer mandated. A straightforward comparison of the radiometric constraints between South African and Huronian sequences indicates that the Makganyene is probably younger than the Gowganda. As the critical interval between them contains the first hints of oxic surface conditions (including the first major red beds and the loss of mass-independent S isotope fractiona-

tion [40,41]), we suggest that the Makganyene Snowball event was triggered by an oxygen-related collapse of the methane greenhouse of Pavlov et al. [42] and Pavlov and Kasting [43].

Acknowledgements

We thank Grant Young for helpful advice on sampling localities; Toru Yasukochi, Robert Kopp, and Takemaru Hirai for assistance in the field work; Vladimir Pavlov, Timothy Raub, and Robert Kopp for critical comments on the manuscript; and Craig Jones and J.P. Cogne for use of paleomagnetic data reduction software. This study was supported by a grant from the NASA Astrobiology Institute and by grants-in-aid for Scientific Research (no. 14403004) of the Japan Society for the Promotion of Science.

References

- [1] D. Evans, Stratigraphic, geochronological, and paleomagnetic constraints upon the Neoproterozoic climatic paradox, *Am. J. Sci.* 300 (5) (2000) 347–433.
- [2] J. Kirschvink, Late Proterozoic low-latitude global glaciation: the Snowball Earth, in: J. Schopf, C. Klein, D. Des Maris (Eds.), *The Proterozoic Biosphere: A Multidisciplinary Study*, Cambridge University Press, Cambridge, UK, 1992, pp. 51–52.
- [3] P. Hoffman, A. Kaufman, G. Halverson, D. Schrag, A Neoproterozoic Snowball Earth, *Science* 281 (5381) (1998) 1342–1346.
- [4] P.F. Hoffman, D.P. Schrag, Snowball Earth, *Sci. Am.* 282 (1) (2000) 68–75.
- [5] D.P. Schrag, P.F. Hoffman, Geophysics—life, geology and Snowball Earth, *Nature* 409 (6818) (2001) 306.
- [6] D. Evans, N. Beukes, J. Kirschvink, Low-latitude glaciation in the Paleoproterozoic, *Nature* 386 (1997) 262–266.
- [7] G. Williams, P. Schmidt, Paleomagnetism of the Paleoproterozoic Gowganda and Lorrain formations, Ontario: low paleolatitude for Huronian glaciation, *Earth Planet. Sci. Lett.* 153 (1997) 157–169.
- [8] P. Schmidt, G. Williams, Paleomagnetism of the Paleoproterozoic hematitic breccia and paleosol at Ville-Marie, Quebec: further evidence for the low paleolatitude of Huronian glaciation, *Earth Planet. Sci. Lett.* 172 (3–4) (1999) 273–285.
- [9] J.L. Kirschvink, E.J. Gaidos, L.E. Bertani, N.J. Beukes, J. Gutzmer, L.N. Maepa, R.E. Steinberger, Paleoproterozoic Snowball Earth: extreme climatic and geochemical global change and its biological consequences, *Proc. Natl. Acad. Sci.* 97 (2000) 1400–1405.
- [10] G.M. Young, Comparative geochemistry of Pleistocene and Paleoproterozoic (Huronian) glaciogenic laminated deposits: relevance to crustal and atmospheric composition in the last 2.3 Ga, *J. Geol.* 109 (4) (2001) 463–477.
- [11] P.F. Hoffman, D.P. Schrag, The Snowball Earth hypothesis: testing the limits of global change, *Terra Nova* 14 (3) (2002) 129–155.
- [12] G.M. Young, D.G.F. Long, C.M. Fedo, H.W. Nesbitt, Paleoproterozoic Huronian basin: product of a Wilson cycle punctuated by glaciations and a meteorite impact, *Sediment. Geol.* 141 (2001) 233–254.
- [13] K.L. Buchan, D.J. Neilson, C.J. Hale, Relative age of Otto stock and Matachewan dykes from paleomagnetism and Implications for the Precambrian polar wander path, *Can. J. Earth Sci.* 27 (7) (1990) 915–922.
- [14] K.L. Buchan, J.K. Mortensen, K.D. Card, J.A. Percival, Paleomagnetism and U–Pb geochronology of diabase dyke swarms of Minto block, Superior Province, Quebec, Canada, *Can. J. Earth Sci.* 35 (9) (1998) 1054–1069.
- [15] H.C. Halls, The Matachewan dyke swarm, Canada—an early Proterozoic magnetic-field reversal, *Earth Planet. Sci. Lett.* 105 (1–3) (1991) 279–292.
- [16] L.M. Heaman, Global mafic magmatism at 2.45 Ga: remnants of an ancient large igneous province? *Geology* 25 (4) (1997) 299–302.
- [17] F. Corfu, A.J. Andrews, A U–Pb age for mineralized Nipissing diabase, Gowganda, Ontario, *Can. J. Earth Sci.* 23 (1) (1986) 107–109.
- [18] D.H. Cornell, S.S. Schutte, B.L. Eglington, The Ongeluk basaltic andesite formation in Griqualand West, South Africa: submarine alteration in a 2222 Ma Proterozoic sea, *Precambrian Res.* 79 (1–2) (1996) 101–123.
- [19] H. Dorland, Provenance, ages, and timing of sedimentation of selected Neoproterozoic and Paleoproterozoic successions on the Kaapvaal Craton, PhD thesis, Rand Afrikaans University (2004).
- [20] G.M. Young, H.W. Nesbitt, The Gowganda Formation in the southern part of the Huronian outcrop belt, Ontario, Canada—stratigraphy, depositional-environments and regional tectonic significance, *Precambrian Res.* 29 (1985) 265–301.
- [21] J. Menzies, Microstructures in diamictites of the lower Gowganda Formation (Huronian), near Elliot Lake, Ontario: evidence for deforming-bed conditions at the grounding line? *J. Sediment. Res.* 70 (1) (2000) 210–216.
- [22] G. Bennett, K.D. Card, K.Y. Tomlinson, The Huronian Supergroup between Sault Ste. Marie and Elliot Lake: evidence for the early Proterozoic atmosphere, climate and tectonics, Institute on Lake Superior Geology 43rd Annual Meeting, Field Trip Guide Book, vol. 43, Institute on Lake Superior Geology, Sudbury, Ontario, Canada, 1997.
- [23] G.M. Young, H.W. Nesbitt, Paleoclimatology and provenance of the glaciogenic Gowganda Formation (Paleoproterozoic), Ontario, Canada: a chemostratigraphic approach, *Geol. Soc. Amer. Bull.* 111 (2) (1999) 264–274.
- [24] L.R. Feng, J.A. Donaldson, H.D. Holland, Alteration rinds on glacial diamictite clasts in the Gowganda Formation: possible indicators of low atmospheric oxygen ca. 2.3 Ga, *Int. Geol. Rev.* 42 (8) (2000) 684–690.

- [25] N. Prasad, S.M. Roscoe, Evidence of anoxic to oxic atmospheric change during 2.45–2.22 Ga from lower and upper sub-Huronian paleosols, Canada, *Catena* 27 (2) (1996) 105–121.
- [26] G.M. Young, The geologic record of glaciation—relevance to the climatic history of Earth, *Geosci. Can.* 18 (3) (1991) 100–108.
- [27] K.L. Buchan, Baked contact test demonstrates primary nature of dominant (N1) magnetization of Nipissing intrusions in Southern Province, Canadian shield, *Earth Planet. Sci. Lett.* 105 (4) (1991) 492–499.
- [28] K.L. Buchan, K.D. Card, F.W. Chandler, Multiple ages of Nipissing diabase intrusion—paleomagnetic evidence from the Englehart area, Ontario, *Can. J. Earth Sci.* 26 (3) (1989) 427–445.
- [29] K.L. Buchan, J.K. Mortensen, K.D. Card, Northeast-trending early Proterozoic dykes of Southern Superior Province—multiple episodes of emplacement recognized from integrated paleomagnetism and U–Pb geochronology, *Can. J. Earth Sci.* 30 (6) (1993) 1286–1296.
- [30] K.L. Buchan, J.K. Mortensen, K.D. Card, Integrated paleomagnetic and U–Pb Geochronological studies of mafic intrusions in the Southern Canadian shield—implications for the early Proterozoic polar wander path, *Precambrian Res.* 69 (1–4) (1994) 1–10.
- [31] P.L. McFadden, M.W. McElhinny, Classification of the reversal test in paleomagnetism, *Geophys. J. Int.* 103 (1990) 725–729.
- [32] N.I. Fisher, T. Lewis, B.J.J. Embleton, *Statistical Analysis of Spherical Data*, Cambridge University Press, Cambridge, 1987, 329 pp.
- [33] J.L. Kirschvink, A new automated sample changer, Spring AGU meeting, EOS, Transactions American Geophysical Union, vol. 83, Southern Canadian shield—implications for the early Proterozoic polar wander path, *Precambrian Res.* 69 (1–4) (1994) 1–10.
- [34] J. Kirschvink, The least-squares line and plane and the analysis of paleomagnetic data, *Geophys. J. R. Astron. Soc.* 62 (3) (1980) 699–718.
- [35] P.W. Schmidt, D.A. Clark, Paleomagnetism and magnetic-anisotropy of Proterozoic banded iron formations and iron-ores of the Hamersley Basin, Western-Australia, *Precambrian Res.* 69 (1–4) (1994) 133–155.
- [36] P.L. McFadden, A new fold test for paleomagnetic studies, *Geophys. J. Int.* 103 (1) (1990) 163–169.
- [37] M. Stupavsky, D.T.A. Symons, Penokean remagnetization of the Basal Huronian Dollyberry Lake Basalts near Elliot Lake, Ontario, *Can. J. Earth Sci.* 20 (1) (1983) 49–56.
- [38] S.M. McLennan, A. Simonetti, S.L. Goldstein, Nd and Pb isotopic evidence for provenance and post-depositional alteration of the Paleoproterozoic Huronian Supergroup, Canada, *Precambrian Res.* 102 (3–4) (2000) 263–278.
- [39] M.J. Frarey, Geology of the Huronian Belt between Sault Ste. Marie and Sudbury, *Mem.-Geol. Surv. Can.* 383 (1977) 87.
- [40] J. Farquhar, H. Bao, M. Thiemens, Atmospheric influence of Earth's earliest sulfur cycle, *Science* 289 (2000) 756–758.
- [41] J. Farquhar, B.A. Wing, Multiple sulfur isotopes and the evolution of the atmosphere, *Earth Planet. Sci. Lett.* 213 (1–2) (2003) 1–13.
- [42] A.A. Pavlov, M.T. Hurtgen, J.F. Kasting, M.A. Arthur, Methane-rich Proterozoic atmosphere? *Geology* 31 (1) (2003) 87–90.
- [43] A.A. Pavlov, J.F. Kasting, Mass-independent fractionation of sulfur isotopes in Archean sediments: strong evidence for an anoxic Archean atmosphere, *Astrobiology* 2 (1) (2002) 27–41.
- [44] R. Butler, *Paleomagnetism: Magnetic Domains to Geologic Terranes*, Blackwell Scientific Publications, Boston, 1992, 319 pp.
- [45] K.L. Buchan, H.C. Halls, J.K. Mortensen, Paleomagnetism, U–Pb geochronology, and geochemistry of Marathon dykes, Superior Province, and comparison with the Fort Frances swarm, *Can. J. Earth Sci.* 33 (12) (1996) 1583–1595.
- [46] M.P. Bates, H.C. Halls, Regional variation in paleomagnetic polarity of the Matachewan dyke swarm related to the Kapuskasing structural zone, Ontario, *Can. J. Earth Sci.* 27 (2) (1990) 200–211.
- [47] H.C. Halls, L.M. Heaman, The paleomagnetic significance of new U–Pb age data from the Molson dyke swarm, Cauchon Lake area, Manitoba, *Can. J. Earth Sci.* 37 (6) (2000) 957–966.
- [48] Y.J. Zhai, H.C. Halls, M.P. Bates, Multiple episodes of dike emplacement along the northwestern margin of the Superior Province, Manitoba, *J. Geophys. Res., [Solid Earth]* 99 (B11) (1994) 21717–21732.